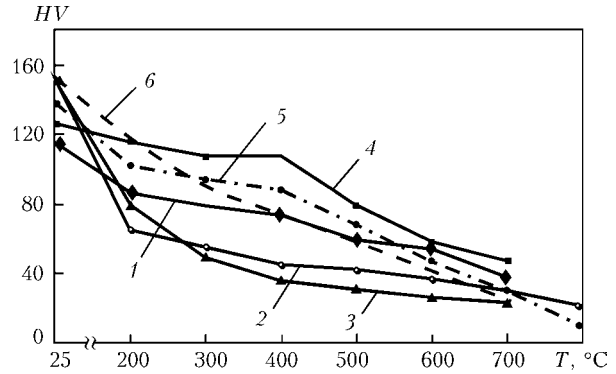

Figure 7. Dependence of hardness of electrodes from different materials on test temperature: *1* — bimetal (surfaced) #30 (PWI); *2* — GlideCop Al-60 (USA); *3* — nanocomposite material S16.102 DISKOM; *4* — bimetal (surfaced) #66 (PWI); *5* — Cu–Cr–Zr (Germany); *6* — BrKhTsr («Krasny Vyborzhets», RF)

ditives, and Figure 6 shows the cellular substructure of the electrode surfaced with wire #66.

As is seen from Figure 7, bimetal (surfaced) electrodes have higher hardness at elevated temperatures. A correlation is found between electrode hardness at elevated temperature and their service durability (see Figures 1 and 7).

To ensure efficiency and stability of the quality of bimetal electrodes it is rational to apply automatic surfacing with solid wire. Improvement of nanocomposite material composition to increase its hardness at elevated temperature is also promising. Such work is currently conducted in cooperation with TsNIIMT DISKOM.

Thus, it is established that electrodes made by arc surfacing and those from nanocomposite material have the highest service durability.

1. Nikolaev, A.K., Rozenberg, V.M. (1978) *Alloys for resistance welding electrodes*. Moscow: Metallurgiya.
2. Nikolaev, A.K., Novikov, A.N., Rozenberg, V.M. (1983) *Chromium bronzes*. Moscow: Metallurgiya.
3. Lipatov, Ya.M. (1975) Components of welding equipment of new dispersion-hardened composites. *Montazhn. i Spets. Raboty v Stroitelstve*, **4**, 11.
4. Daneliya, E.P., Rozenberg, V.M. (1979) *Internally oxidized alloys*. Moscow: Metallurgiya.
5. Shalunov, E.P., Ravitsky, G., Berent, V.Ya. (2003) Long-life electrodes for resistance welding made of copper dispersion-hardened composites: development, production, application. In: *Proc. of Int. Conf. on Electric Contacts and Electrodes* (Katsiveli, Crimea, 15–21 Sept. 2003). Kiev: IPM, 89–92.
6. Shalunov, E.P., Davydenkov, V.A. (2004) Long-life electrodes for resistance welding of copper composites. In: *Transact. of I.N. Frantsevich IPMS on Electric Contacts and Electrodes*. Kiev: IPM, 190–201.
7. *TU U 20113410.001–98*: Dispersion-hardened materials for electric contact. Specifications. Introd. 02.06.98.
8. Movchan, B.A., Osokin, V.A., Grechanyuk, N.I. et al. (1991) Structure, mechanical properties and thermal stability of condensed dispersion-hardened materials Cu–Y–Mo. Report 1. *Problemy Spets. Elektrometallurgii*, **4**, 27–32.
9. Anoshin, V.A., Ilyushenko, V.M., Podola, N.V. et al. (2003) Bimetal electrodes for resistance spot welding of steels with anticorrosive coating. In: *Abstr. of Int. Conf.* on *Current Problems of Welding and Service Life of Coatings* (Kiev, 24–27 Nov. 2003). Kiev: PWI, 6–7.
10. Yavorsky, Yu.D., Zelmanovich, V.Ya. (1966) Spot and seam resistance welding of low-carbon steels with protective coatings. *Avtomatich. Svarka*, **6**, 59–63.
11. Bochvar, A.A. (1956) *Physical metallurgy*. Moscow: Metallurgizdat.

INFLUENCE OF GETTER ADDITIVES ON HYDROGEN EMBRITTLEMENT OF WELDED JOINTS OF STRUCTURAL MATERIALS OF NPP EQUIPMENT

V.M. AZHAZHA, S.D. LAVRINENKO, G.D. TOLSTOLUTSKAYA, N.N. PILIPENKO, Yu.P. BOBROV, A.P. SVINARENKO and **A.N. AKSENOVA**

National Science Center «Kharkov Institute of Physics and Technology», NASU, Kharkov, Ukraine

The paper gives analysis of literature data on searching for getter materials, which can be recommended for creation of hydrogen traps by introducing them into structural materials and welded joints of NPP equipment. Hydride-forming alloys and compounds based on zirconium, titanium and vanadium are considered as the most promising ones. Rare-earth metals and their alloys, binary compounds of rare-earth metals with transition metals of VIII group are proposed as materials of getter additives to create hydrogen traps in structural materials and welded joints of NPP equipment.

Keywords: *structural materials, service life, physical simulation, weld metal, hydrogen, getter additives, nuclear-physics research*

Hydrogen is known to be one of the most harmful and hazardous impurities in metals and alloys. Practical experience and almost all experimental investigations of hydrogen influence on the processes of embrittlement, strengthening, long-term strength and thermal stability, static and cyclic fatigue, fatigue strength, fatigue resistance, creep in metals and alloys reveal its negative role in these processes. A sufficiently high content of hydrogen in structural materials under certain operation conditions can lead to significant embrittlement of these materials, and, as a result, mark-

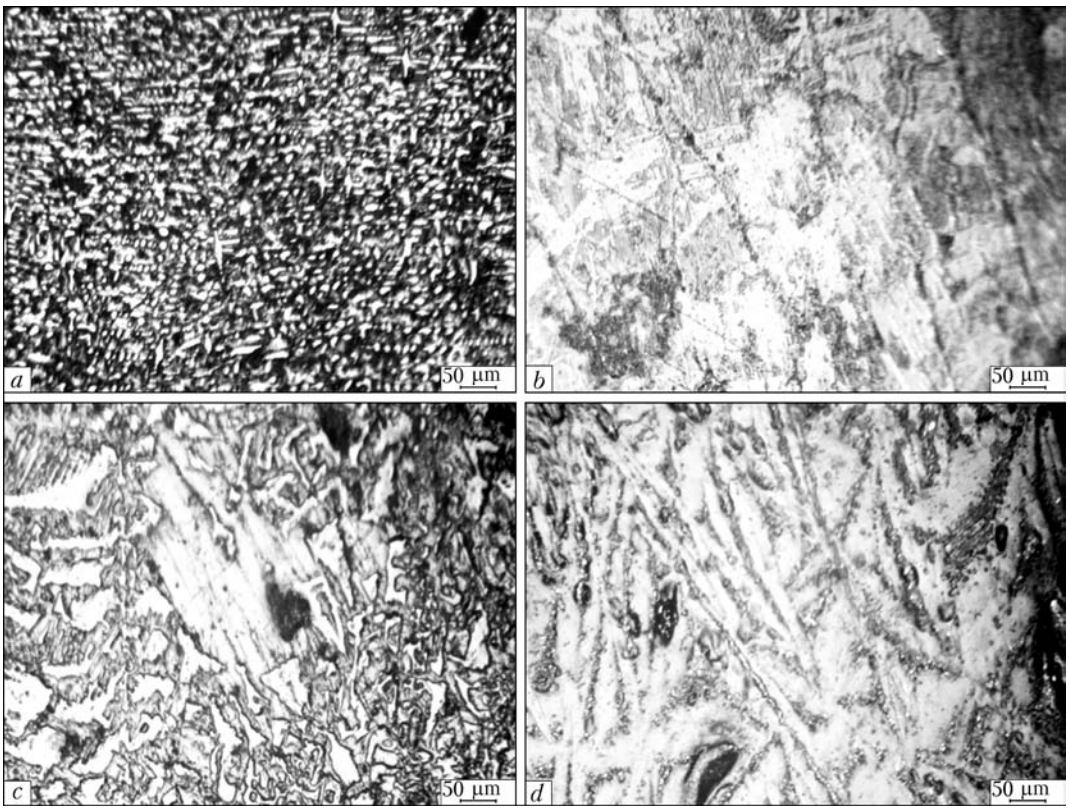

Figure 1. Microstructures of ingots of Fe–Y system alloys of different compositions: *a* — Fe90–Y10; *b* — Fe85–Y65; *c* — Fe65–Y35; *d* — Fe57–Y43

edly impair their performance, up to complete inoperability.

The weld and adjacent zone often are some of the most critical parts of the structural material. Performance degradation through embrittlement in many cases is associated with hydrogen dissolved in the weld metal. At present all the data on hydrogen behaviour in metal and alloys provide grounds for connecting the mechanisms of their hydrogen embrittlement with hydrogen interaction with their microstructural inhomogeneity: dissolved foreign atoms, vacancies, dislocations, grain and phase boundaries, phase precipitates, micro- and macropores, microcracks, inclusions of foreign particles, etc. Therefore, alongside the traditional method of reducing the probability of hydrogen embrittlement consisting in reduction of hydrogen concentration both in welding consumables and in the atmosphere, in which the welding process proceeds, other methods of embrittlement prevention through control of parameters of processes of hydrogen diffusion in the welded joint and structural material are also of interest.

Getter materials. Proceeding from the above analysis of getter materials from the viewpoint of their application as potential materials of getter additives, two series of alloys (based on Fe–Y binary and Zr–Co–Y ternary systems) were selected, which have the following initial compositions, wt.%: Fe90–Y10; Zr80.8–Co14.2–Y5; Fe85–Y15; Zr82.28–Co17.72; Fe65–Y35; Zr66.1–Co17.8–Y16.1; Fe57–Y43; Zr75.53–Co13.95–Y10.52.

Alloys of Fe–Y and Zr–Co–Y system are produced by argon-arc melting by nonconsumable (tungsten) electrode in high-purity argon atmosphere. To achieve a uniform distribution of component elements, alloy ingots were remelted several times. High-purity iron of multiple electron beam remelting, iodide zirconium, electrolytic cobalt and yttrium of 99.9 % purity were used as initial elements.

X-ray structural and metallographic analyses were applied to study the alloy phase composition and their structure. Phase composition of the produced alloys was determined by X-ray method in DRON-2M diffractometer in filtered Cu_{K_α}-radiation. Metallorgaphic investigations were conducted in MIM-8 microscope. The alloy microhardness was determined in MVT-3 microhardness meter, measurement error being ±5 %.

Prior to investigations the sample surface was ground with abrasive paper and polished with diamond paste.

For Fe–Y system alloys, 5 % solution of nitric acid in ethyl alcohol (nital) was used, and for alloys of Zr–Co–Y system, etchant of the following composition was applied: 15.4 ml HF; 17.3 ml HNO_3; 17.3 ml H_2SO_4; and 50 ml of distilled water. H_2SO_3 acid was added to the etchant for grinding the surface of samples, which was coated by passivating film during the etching process.

Mass spectrometric analysis was applied to study the gas evolution spectra [1], using MX-7203 mass-spectrometer. It is designed for hydrogen detection, as well as control of gas impurities in metals and

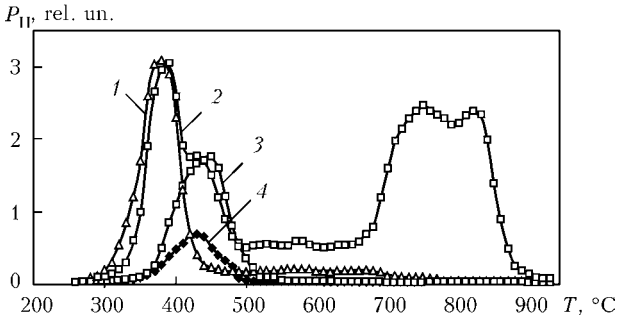

Figure 2. Variation of partial pressure of hydrogen P_H at heating in vacuum of samples of Fe–Y system alloys after hydrogen saturation at the temperature of 350 °C for 8 h: *1* — Fe85–Y15; *2* — Fe57–Y43; *3* — Fe65–Y35; *4* — Fe90–Y10

alloys, which evolve from them at heating (gases with up to 60 mass numbers are detected).

Alloy hydrogenation was conducted at the temperature of 350 °C for 8 h. Hydrogen gas evolution from the alloys before and after hydrogenation occurred at temperature rise from room temperature up to 950 °C.

According to the equilibrium diagram of Fe–Y system [2], the studied alloys are two-phase materials. Fe90–Y10 and Fe85–Y15 alloys contain α-Fe(Y) + $Fe_{17}Y_2$ phases. Assessment by the rule of segments gives their ratio as 38 and 62 % and 5 and 95 %, respectively. Alloys Fe65–Y35 and Fe57–Y43 consist of two intermetallics Fe_3Y + Fe_2Y and, according to assessment by the same rule, they have the ratio of 96 and 4 %, 14 and 86 %, respectively. Figure 1 gives microstructures of ingot surfaces of Fe–Y system alloys of the above compositions.

Quantitative ratio of phases assessed metallographically, is in agreement with earlier obtained results. Values of microhardness for alloys with increasing yttrium content are equal to 4270, 7700, 6700 and 5740 MPa, respectively.

Thermal desorption from the alloys reflects the total effect of gas evolution from phases present in them and hydrogenolysis products formed in alloy production and heating. Curves of hydrogen evolution at heating in vacuum of samples of Fe–Y system alloys are shown in Figure 2. The shape of the curves is determined, mainly, by the content of hydrogen present in the alloy phases, its redistribution in them at temperature variation, degree of hydrogen solubility and its equilibrium pressure above the alloy components.

In Fe90–Y10 and Fe85–Y15 alloys the nature of thermal desorption depends predominantly on the content of $Fe_{17}Y_2$ phase in them. Data of Figure 2 are in agreement with the data on thermal desorption of hydrogen from this phase given in [3, 4].

Curves of thermal desorption of Fe65–Y35 and Fe57–Y43 alloys, which contain Fe_3Y and Fe_2Y phases, represent the complex transformations occurring with their hydrides at temperature variation, which is not contradictory to the data of [5, 6].

Analysis of the obtained thermal desorption curves, as well as concentration of absorbed hydrogen, given in the Table, showed that Fe57–Y43 alloy, compared to other alloys of Fe–Y system, absorbs the largest amount of hydrogen and retains it up to higher temperature values (approximately 900 °C and higher).

Data of metallography and X-ray structural analysis of alloys of Zr–Co–Y system showed that Zr82.3–Co17.7 binary alloy is a single-phase alloy and consists of ZrCo intermetallic with rhombic lattice parameters a = 8.945 (Δ = 0.002); b = 10.875 (Δ =0.013); c = = 3.270 (Δ = 0.003) and elementary cell volume V = = 318,10 (Δ = 0.740), which is in good agreement with the data of [7].

Zr80.8–Co14.2–Y5 alloy consists of three phases (ZrCo, α-Zr and α-Y), having the following crystallographic parameters, respectively: a = 8.915 (Δ = = 0.250), b = 10.914 (Δ = 0.030), c = 3.298 (Δ = = 0.019) and V = 320.92 (Δ = 3.820); a = 3.238 (Δ = = 0.003), c = 5.161 (Δ = 0.001); a = 3.649 (Δ = 0.004), c = 5.752 (Δ = 0.030).

Zr75.5–Co14–Y10.5 alloy consists of the same phases as the previous alloy, and these phases have the following parameters, respectively: a = 8.932 (Δ = = 0.008), b = 10.955 (Δ = 0.400), c = 3.273 (Δ =

Hydrogen content in alloy samples before and after their saturation with hydrogen at 350 °C temperature for 8 h

Systems	Alloy	Hydrogen concentration in initial alloys		Hydrogen concentration in alloys after their hydrogen saturation at temperature of 350 °C	
		cm^3/100 g	%	cm^3/100 g	%
Fe–Y	Fe90–Y10	89	0.008	1400	0.13
	Fe85–Y15	46	0.004	3300	0.30
	Fe65–Y35	64	0.006	6700	0.60
	Fe57–Y43	138	0.012	15300	1.38
Zr–Co–Y	Zr82.3–Co17.7	81	0.007	14100	1.27
	Zr80.8–Co14.2–Y5	106	0.010	22400	2.02
	Zr75.5–Co14–Y10.5	206	0.020	22800	2.05
	Zr66.1–Co17.8–Y16.1	170	0.015	16400	1.48

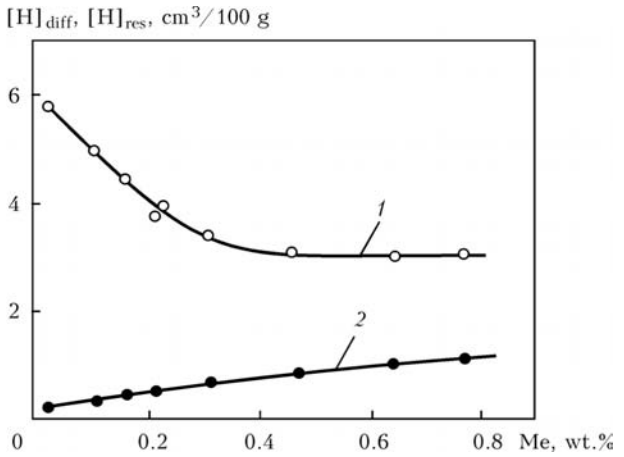

Figure 3. Influence of REE in electrode coating on concentration of diffusible (*1*) and residual (*2*) hydrogen [11]

= 0.001) and V = 320.23 (Δ = 1.560); a = 3.231 (Δ = = 0.004), c = 5.161 (Δ = 0.004); a = 3.652 (Δ = 0.005), c = 5.735 (Δ = 0.020).

In Zr66.1–Co17.8–Y16.1 alloy only Zr_3Co phase of the three metallographically detected phases was definitely identified.

Complex profiles of thermal desorption curves of Zr–Co–Y system alloys, which have been subjected to hydrogenation, are indicative of the fact that quite significant structural changes proceed in them at temperature change. Hydrogen gas evolution from these alloys occurs practically in the entire studied temperature range, and for Zr75.5–Co14–Y10.5 alloy it does not stop at maximum temperature of about 950 °C. Tabulated data show that of all the alloys of Zr–Co–Y system studied in this work, this alloy absorbs and retains the largest fraction of hydrogen.

Additives of rare-earth elements (REE) with a high affinity to gas and other interstitial elements, lead to a change in the properties of metals and alloys. Presence of an even small amount of yttrium, lanthanum, scandium, and cesium in the solid solution noticeably changes the diffusion mobility of atoms, elastic fields of dislocations and interfaces, and, therefore, the nature and kinetics of precipitates. Of special interest

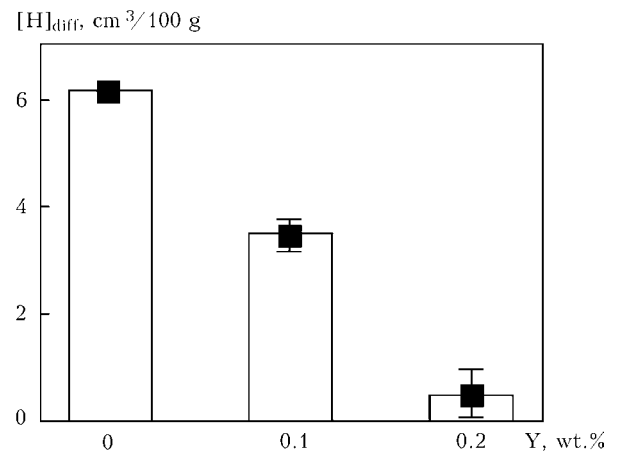

Figure 4. Influence of weight fraction of yttrium inside the powder wires (electrodes) on diffusible hydrogen concentration in the metal of weld made by welding in a mixture of gases of Ar + 0.1 % H_2 [11]

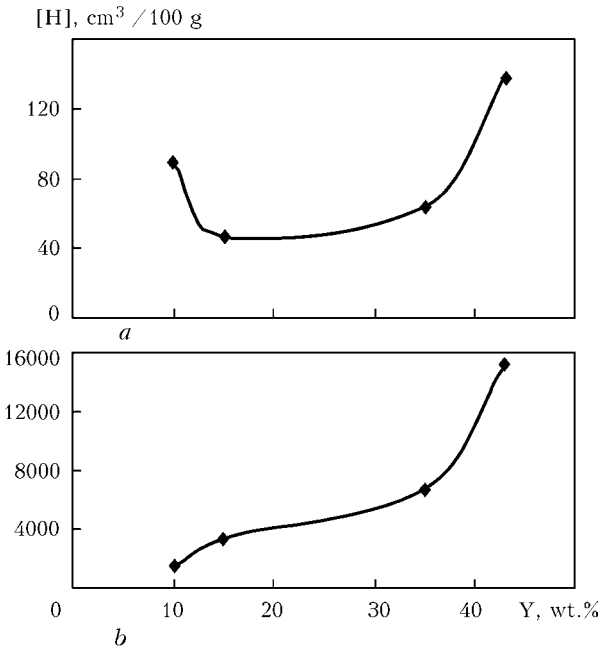

Figure 5. Concentration of hydrogen evolving from samples of alloys of Fe–Y system before (*a*) and after (*b*) their hydrogenation

is investigation of the influence of REE on evolution of structural-phase state and resistance of materials at irradiation. REE impact on radiation resistance depends on their concentration, presence of gas impurities in the solid solution and other factors. Positive influence of REE microalloying is attributable to increased density of the centers of secondary phase formation and more intensive decomposition of initial metastable solid solution [8, 9].

It should be noted that pure REE are relatively expensive. Moreover, alloying of radiation-resistant steels and alloys runs into technological difficulties associated with ensuring their uniform distribution in the solid solution, where their action on radiation

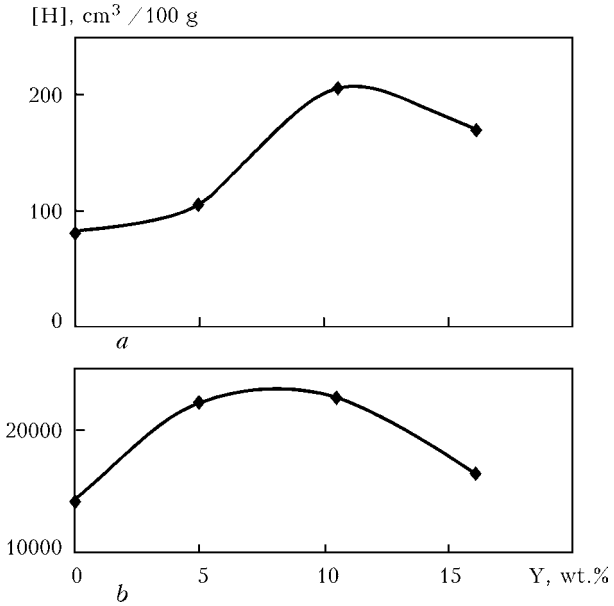

Figure 6. Concentration of hydrogen evolving from samples of alloys of Zr–Co–Y system before (*a*) and after (*b*) their hydrogenation

resistance is optimum [8, 9]. In alloy production they practically do not come to the metal because of the high reactivity of REE interaction with the slag covering the melt. Moreover, REE have a high vapour pressure [10], and scandium also has low density. Therefore, at addition in the pure form (even in the shielding atmosphere), their consumption is unreasonably high. From the view point of material saving, manufacturing of REE master alloys from their chemical compounds by metallothermal reduction is practicable.

In the work it is shown that REE additives in the weld metal lead to reduction of the fraction of diffusible hydrogen in it (Figures 3 and 4), as they bind hydrogen, thus freeing the alloy matrix.

Change of concentration of hydrogen, which evolved from the samples of Fe–Y alloys before and after their hydrogenation, is shown in Figure 5. It is seen that increase of yttrium content in the alloy lead to an increase of absorbed hydrogen concentration, that is particularly noticeable after hydrogenation of these alloys.

Concentration of hydrogen evolving from samples of alloys of Zr–Co–Y system before and after their hydrogenation is shown in Figure 6. It is seen from the Figure that hydrogen concentration is maximum at yttrium content between 5 and 10 wt.%, and it decreases with increase of yttrium content to 15 wt.%.

Model welds with getter additives. Model samples of alloys simulating welds with special getter additives in it, capable of effective absorption, accumulation and retention of hydrogen, were made for investigations. These alloys consists of 95 wt.% Fe and 5 % of additive of Fe–Y system intermetallics. Intermetallic additives had the following compositions, wt.%: Fe90–Y10; Fe85–Y15; Fe65–Y35; Fe57–Y43.

Proceeding from metallographic analysis of sample surface, it was determined that alloys of the studied compositions consist of two phases — Fe(FeY) and FeY + Fe. Distribution of added intermetallic in iron proceeds uniformly over the entire volume. Grains of one phase take up a much larger surface of the section, and the other phase is located between the grains of the first phase in the form of thin interlayers and forms a kind of frame. Figure 7 gives the microstructures of alloy sample surface.

Microstructures of surfaces of model alloys with getter additives, containing 10 and 25 wt.% Y are similar, and microstructures of surfaces of alloys with getter additives with 35 and 43 wt.% Y are also similar, which is attributable to the difference in phase composition in the first and second case. Microhardness value in Fe(FeY) phase of these alloys (at increase of yttrium content in the getter additive) is equal to 1250, 1280, 1210 and 1270 MPa.

Curve *1* in Figure 8 is characterized by a complex profile, noticeable evolution of hydrogen starts at the temperature of approximately 300 °C and ends at 900 °C; curve *2* has a maximum at the temperature of about 600 °C, main evolution of hydrogen occurs at the temperature from 400 up to 900 °C.

Results of hydrogen thermal desorption from an alloy with getter additive containing 10 wt.% Y (see

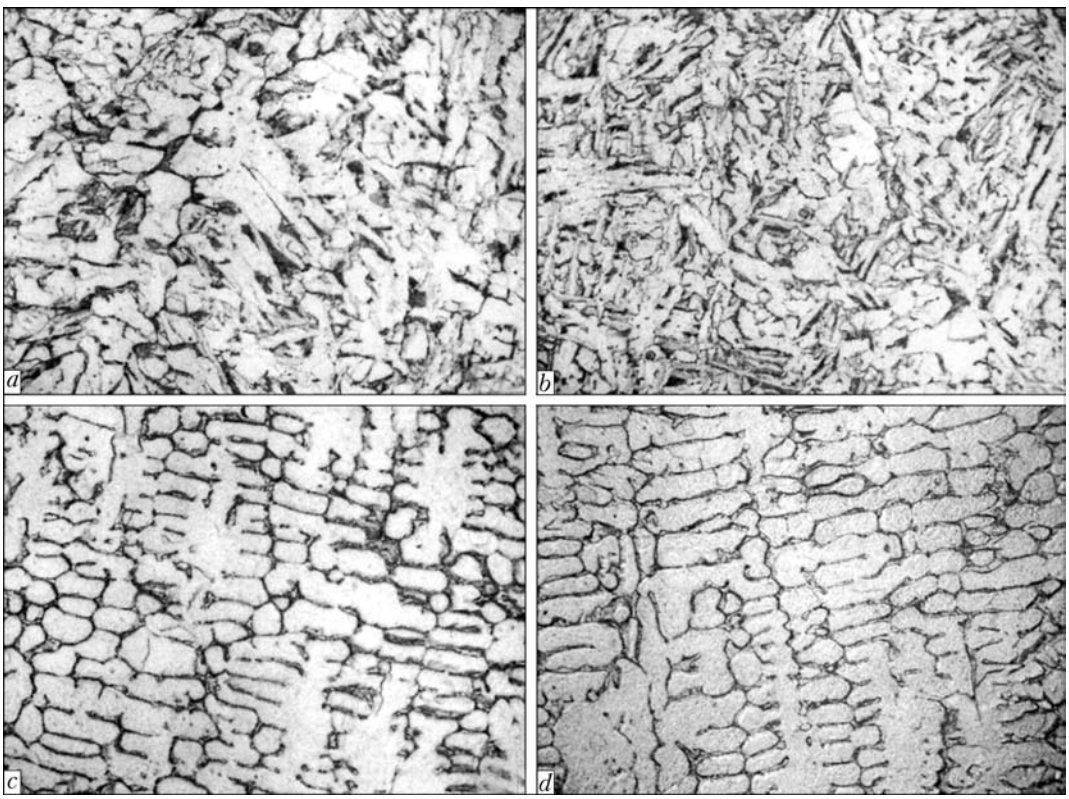

Figure 7. Microstructures (×300) of the surface of samples of alloys with getter additives containing 10 (*a*), 15 (*b*), 35 (*c*) and 43 (*d*) wt.% Y

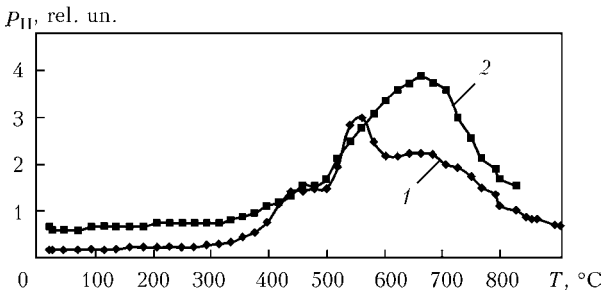

Figure 8. Change of partial pressure of hydrogen P_H at heating in vacuum of samples of an alloy with getter additive with 10 wt.% Y before (*1*) and after (*2*) hydrogenation

Figure 8), are in agreement with the data of investigation of hydrogen thermal desorption from Fe90–Y10 alloy [12], and do not disagree with the data on hydrogen thermal desorption from $Fe_{17}Y_2$ intermetallic, given in [13]. View of curve *2* and absolute value of the observed peak of hydrogen desorption, similar to our case, is influenced by the nature of hydrogen diffusion through the iron matrix. Iron content can significantly affect hydrogen diffusion and amplitude of the observed thermal desorption peaks [14].

Nuclear-physical investigation of distribution of hydrogen and its isotopes in new type of model welds. Sample saturation with deuterium was performed in Implantator unit with an oilfree pumping down system, ensuring the residual gas pressure in the target chamber on the level of $(2–3)\cdot10^{-4}$ Pa. Samples were irradiated by deuterium ions D^{2+} with energy E = 10 keV (5 keV/D^+) up to the dose of $(0.5–4.0)\cdot10^{16}$ D/cm^2.

Samples were annealed at the temperature of 300–1200 °C with direct current passage at the rate of temperature rise and drop of 7 K/s^{-1}.

After irradiation distribution of implanted particles by depth was measured through nuclear reaction D(^{3}He, p)^{4}He using ^{3}He (E = 700 keV) beams. Measurements were performed in electrostatic accelerator ESU-2 in direct scattering geometry, ^{3}He ion beam hit the sample surface at an angle of 30°, and nuclear reaction products were recorded at 60° angle to the analyzed beam. Beam diameter at irradiation was 3 mm, and at analysis it was 2 mm. Division by penetration depth in direct scattering geometry was equal to 30 nm. This procedure is described in greater detail in [15].

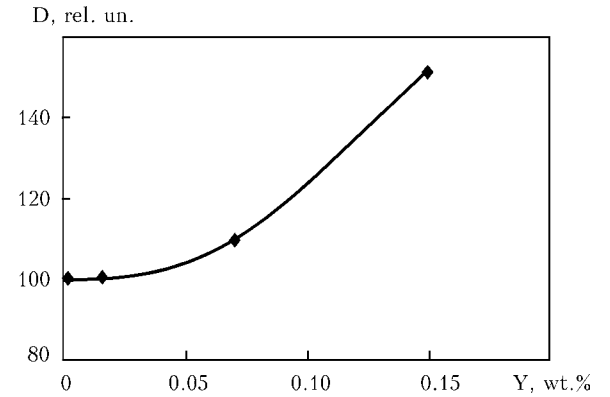

Figure 9. Content of deuterium D evolved from samples with added yttrium after exposure to ions D^{2+} with 12 keV energy up to the dose of $5\cdot10^{16}$ D/cm^2

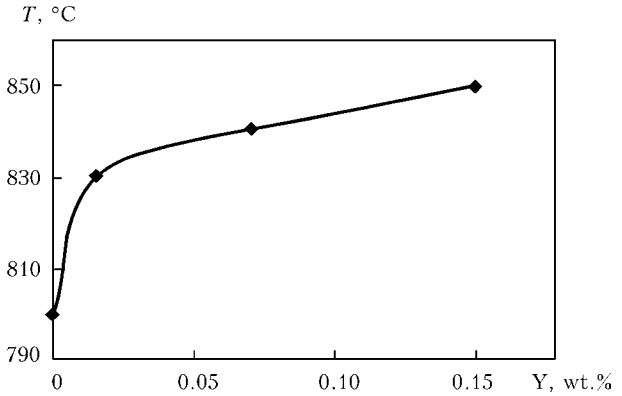

Figure 10. Temperature influence on maximum gas evolution of hydrogen from model weld metal with varying content of added yttrium

Content of deuterium, which has evolved after exposure to D^{2+} with 12 keV energy up to the dose of $5\cdot10^{16}$ D/cm^2 from samples of alloys with yttrium additives, is shown in Figure 9, from which it is seen that at increased content of yttrium added to the alloy, the content of evolving deuterium becomes higher. This is indicative of the fact that at saturation of weld metal with deuterium, it behaves as a residual element (compared to Figure 3).

Method of mass-spectrometry analysis was used to study the temperature interval of hydrogen gas evolution, depending on added yttrium content. Figure 10 shows that with increase of yttrium content in model weld metal, the temperature at which maximum evolution of hydrogen gas occurs, shifts towards high temperature region. This is indicative of the fact that at high yttrium content hydrogen is retained stronger in the model weld metal.

As is seen from Figure 11, concentration of evolved hydrogen decreases with increase of added yttrium content. This shows that absorbed hydrogen is retained by yttrium in model weld metal, i.e. is diffus-

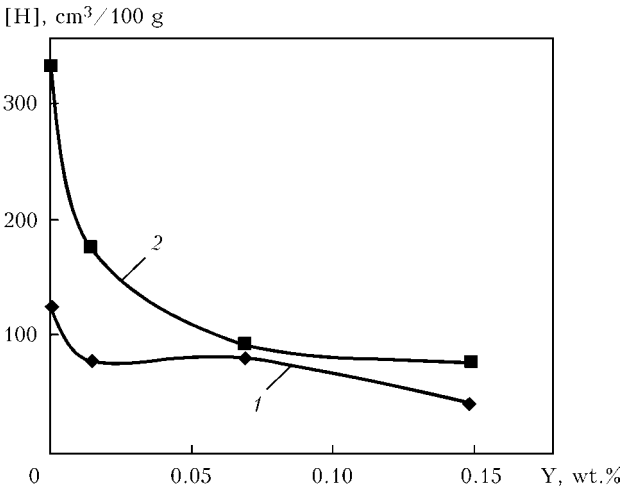

Figure 11. Variation of concentration of hydrogen evolving from model weld metal depending on concentration of added yttrium in the initial condition (*1*) and after hydrogenation (*2*)

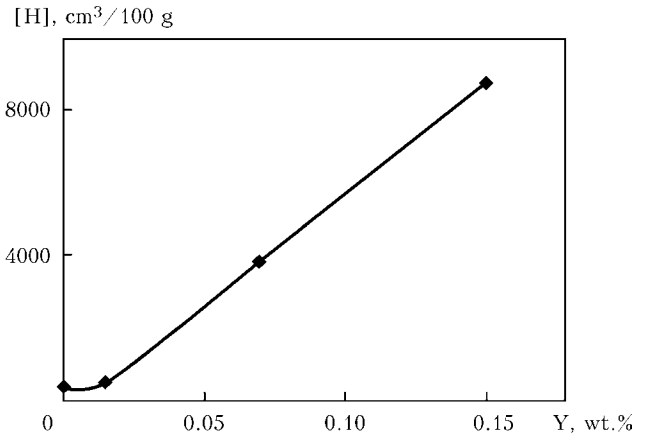

Figure 12. Change of concentration of hydrogen evolving from model weld metal depending on added yttrium content before and after hydrogenation

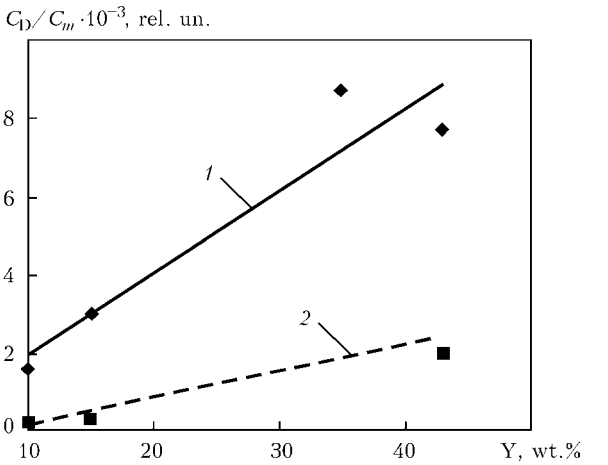

Figure 14. Influence of yttrium content in model weld metal on surface concentration (*1*) and concentration of ion-implanted deuterium at the depth of 0.5–1.8 μm (*2*) at room temperature with 6 keV energy up to the dose of $5 \cdot 10^{16}$ D/cm^2

ible. At longer time of saturation of model weld metal by hydrogen, concentration of absorbed hydrogen in yttrium rises (Figure 12).

Comparison of Figure 9 and Figure 12 may reveal the following regularity: concentration of evolved deuterium and yttrium occurs with increase of yttrium content. It is possible that there is a limit concentration of hydrogen (deuterium), starting from which the mechanism of hydrogen (deuterium) retention by yttrium changes, with hydrogen changing from diffusible to residual.

Figure 13 shows the spatial-concentrational distribution of deuterium by depth d of the layer, on which it is implanted (it is changed by the above procedure), in the metal of model welds with different yttrium content.

Curve of variation of deuterium content is a drooping one with about 200 nm half-width. The main part of entrapped deuterium is concentrated in this region. Part of the remaining implanted gas is uniformly distributed in the lattices to the maximum depth of

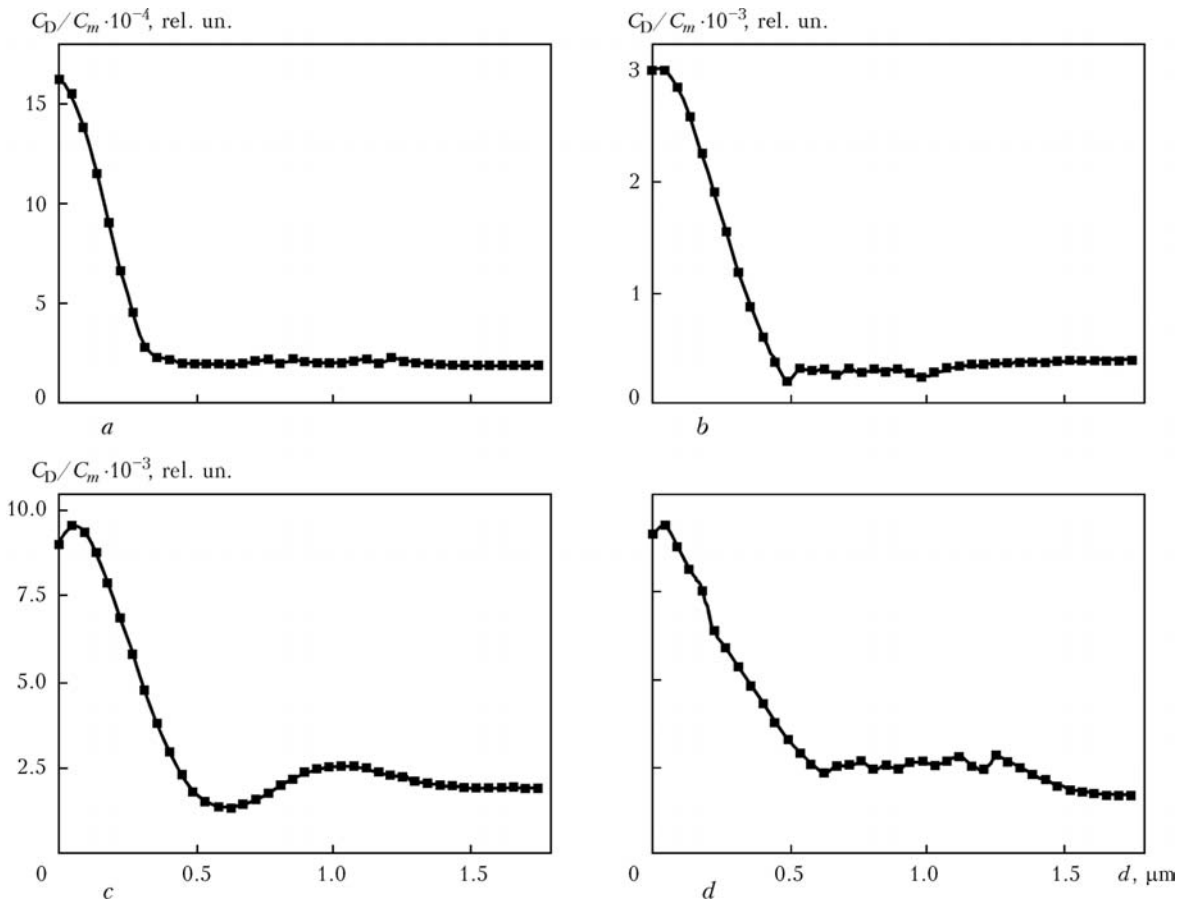

Figure 13. Distribution by depth of deuterium (C_D/C_m — ratio of deuterium atoms to matrix atoms) ion-implanted at room temperature with 6 keV energy to the dose of $5 \cdot 10^{16}$ D/cm^2 in the metal of model welds with 10 (*a*), 15 (*b*), 35 (*c*) and 43 (*d*) wt.% Y

1.8 μm, at which analysis of ^{3}He was performed in model welds at 1.4 MeV energy. Deuterium penetration to depths greatly exceeding its path length is, apparently, due to saturation of penetration layer and appearance of highly mobile gas component, capable of freely migrating to sample depth.

All the components of deuterium distribution in model weld metal (namely, its content on the surface and in the penetration layer, in the «tail» of distribution and total content of deuterium retained in the samples) increase practically linearly with increase of yttrium content in the weld metal (Figure 14). Deuterium accumulation becomes higher in samples of model welds with higher content of getter additive.

Thus, a series of alloys of Fe–Y and Zr–Co–Y system of different composition was produced. Their phase composition and thermal desorption properties were studied. It is shown that these alloys are characterized by a sufficiently high temperature of hydrogen retention and, therefore, can be considered as materials for getter additives to create hydrogen traps in structural materials and welded joints of NPP equipment, promoting an improvement of their service properties by reducing hydrogen influence.

Concentration of hydrogen evolving from getter additives of Zr–Y system rises with increase of added yttrium content.

A series of model welds of joints with different content of getter additives was produced. It is shown that concentration of hydrogen evolving from weld metal decreases with increase of yttrium content in the getter additive. This is indicative of the fact that the absorbed hydrogen is retained by yttrium in model weld metal.

Nuclear-physical investigations of distribution of hydrogen and its isotopes in the metal of new type of model welds were performed. Spatial-concentrational distribution of deuterium in model weld metal showed that content of absorbed deuterium rises with increases of yttrium content.

1. Azhazha, V.M., Bobrov, Yu.P., Bovda, A.M. et al. (2006) Examination of gas emission in vacuum heating of hydrogenated alloy Nd–Fe–B. *Voprosy Atomn. Nauki i Tekhniki. Vakuum, Pure Metals, Superconductors Series*, **1**, 156–159.
2. (1996) *Constitutional diagrams of binary metallic systems*: Refer. Book. Ed. by N.P. Lyakishev. Vol. 1. Moscow: Mashinostroenie.
3. Wirth, S., Skomski, R., Coey, J.M.D. (1998) Hydrogen in R_2Fe_{17} intermetallic compounds. In: *Structural, thermodynamics and magnetic properties: Res. Pap. Phys. Astronomy*, 55(**9**), 5700–5707.
4. Nikitin, S.A., Ovchenkov, E.A., Tereshina, I.S. et al. (1998) Synthesis of ternary hydrides and nitrides R_2Fe_{17} (R–Y, Tb, Dy, Ho, Er) and effect of interstitial elements (H_2, N_2) on magnetic anisotropy and magnetostriction. *Metally*, **2**, 111–116.
5. Kolachev, B.A., Shalin, R.E., Iliin, A.A. (1995) *Hydrogen-accumulating alloys*: Refer. Book. Moscow: Metallurgiya.
6. Leblond, T., Paul-Boncour, V., Cuevas, F. et al. (2009) Fernandez study of the multipeak deuterium thermodesorption in YFe_2D_x ($1.3 < x < 4.2$) by DSC, TD and in situ neutron diffraction. *Int. J. Hydrogen Energy*, 34, Issue 5, 11–14.
7. (1996) *Data base PCPDF*. Int. Center for Diffraction Data, 20–23.
8. Zelensky, V.F., Neklyudov, I.M. (1991) Effect of rare-earth elements on radiation resistance of materials. In: *Proc. of Int. Conf. on Radiation Materials Science* (Kharkov, Sept. 1991). Vol. 2. Kharkov, 45–57.
9. Bakaj, A.S., Gann, V.V., Zelensky, V.F. et al. (1990) Alternative polarity recombination centers of point defects. *Effects of Radiation on Materials*, **1**, 623–631.
10. Savitsky, E.M., Burkhanov, G.S. (1980) *Rare metals and alloys. Physico-chemical analysis and materials science*. Moscow: Nauka.
11. Pokhodnya, I.K., Yavdoshchin, I.R., Paltsevich, A.P. et al. (2004) *Metallurgy of arc welding. Interaction of metal with gases*. Kiev: Naukova Dumka.
12. Azhazha, V.M., Lavrinenko, S.D., Svinarenko, A.P. et al. (2009) Getter alloys for creation of hydrogen traps in structural materials and welded joints of nuclear power plant equipment. *Voprosy Atomn. Nauki i Tekhniki. Vakuum, Pure Metals, Superconductors Series*, **6**, 127–133.
13. Skomski, R. (2006) Hydrogen in R_2Fe_{17} intermetallic compounds. In: *Structural, thermodynamics and magnetic properties: Res. Pap. Phys. Astronomy*, 5700–5707.
14. Kakinichi, K., Itagaki, N., Furuya, T. et al. (2004) Role of iron for hydrogen absorption mechanism in zirconium alloys. *J. ASTM Int.*, 1(**10**), 349–365.
15. Karpov, S.A., Kopanets, I.E., Neklyudov, I.M. et al. (2004) Combination of method of nuclear reactions, thermodesorption spectrometry and double-beam radiation during investigation of helium and hydrogen behavior in structural materials. In: P*roc. of 14th Int. Meeting on Radiation Physics of Solid* (Sevastopol, 5–10 July 2004). Sevastopol, 592–596.